J. Electroanal. Chem., 300 (1991) 447–465
Elsevier Sequoia S.A., Lausanne

In situ second harmonic generation studies of chemisorption at well-ordered Pt(111) electrodes in perchloric acid solutions

Matthew L. Lynch, Barbara J. Barner and Robert M. Corn

Department of Chemistry, University of Wisconsin-Madison, 1101 University Ave., Madison, WI 53706 (USA)

(Received 15 May 1990; in revised form 15 June 1990)

Abstract

The technique of optical second harmonic generation (SHG) is used an in situ probe of chemisorption and structure at flame-annealed Pt(111) electrodes in perchloric acid solutions. Rotational anisotropy SHG measurements demonstrate that the single crystal surface order is preserved when the electrodes are transferred to solution with an iodine overlayer and cleaned through an iodine-CO exchange reaction and subsequent CO oxidation electrochemistry. The chemisorption of both iodine and CO produces an anisotropic response from the surface with a reduced average surface symmetry due to the presence of the adsorbed overlayer. The SHG signal from the well-ordered Pt(111) surface in perchloric acid after the removal of the CO also reveals the presence of an ordered chemisorbed overlayer at all electrode potentials negative of the butterfly peaks. Although the identity of the chemisorbed species cannot be determined unambiguously from the SHG measurements, comparisons with the potential dependent SHG response from Pt(100) and polycrystalline platinum electrodes relate the SHG signal in this potential range to an ordered overlayer of a hydrogen species. The SHG measurements also confirm the electrochemical evidence that these ordered structures are modified upon the disruption of the longer range domain structure of the well-ordered Pt(111) surface.

INTRODUCTION

The structure of the well-ordered Pt(111) single crystal electrochemical interface in acidic media remains a subject of great interest and controversy for both theoretical and practical reasons. The original report by Clavilier [1] and the subsequent confirmation [2] of anomalous voltammetry for the hydrogen and oxygen electrosorption processes at this electrode overturned the previous structural model of what had appeared to be a prototypical electrochemical interface [3–6]. In an effort to identify the structures present at this electrode, a number of research

0022-0728/91/$03.50

groups have performed both ex situ [7–9] and in situ [10,11] spectroscopic measurements on this surface. Three major conclusions have been reached by various authors concerning the Pt(111) electrode: (i) there is a long range ordering process that is responsible for the unusual voltammetry on these electrodes, (ii) the deposition of atomic hydrogen is quite different on the well-ordered Pt(111) surfaces as compared to disordered Pt(111) and polycrystalline electrodes, and (iii) at positive potentials there appears to be the formation of an OH or other oxygen species that is not present on disordered Pt(111) and polycrystalline electrodes. In an effort to create a coherent model of this interface, Ross has suggested that a lattice match of the Pt(111) surface and the hydrogen bonding of the inner layer water molecules and hydronium ions leads to an unusually stable surface structure that is responsible for the anomalous voltammetry [12,13].

In addition to the interesting theoretical reasons for understanding this electrochemical interface, there is a practical reason for the characterization of the Pt(111) electrode. The Pt(111) crystal face is a very stable surface that can be prepared by flame-annealing processes such as those employed by Clavilier [1], and by other groups [14–17]. In particular, the flame annealing methodology introduced by Zurwaski et al. [14] using iodine and CO protective overlayers has been shown to provide a reliable route for the preparation of well-ordered, single crystal electrochemical surfaces without the need for UHV technology. Both electrochemical studies and careful emersion studies of the electrodes with UHV techniques have shown that the flame annealed Pt(111) surfaces are indeed well-ordered [9]. The preparation of such well-defined surfaces is an essential first step for the study of fundamental heterogeneous electrochemical processes such as underpotential deposition [18,19] and catalytic oxidation [5,20]. The ability to create well-ordered surfaces without UHV technology is greatly accelerating the research efforts in these areas.

Thus for both theoretical and practical reasons it is of interest to identify the ordered chemisorbate structures that are present on the Pt(111) surface when in an electrochemical environment. Since these structures might not survive emersion into UHV, it is necessary to employ an in situ method to identify the species present at the surface. As mentioned above, in situ electroreflectance and specular reflectance measurements have already provided information on the chemical species present on this surface [10]. The technique of optical second harmonic generation (SHG) is a complementary surface sensitive optical method that can be used to monitor the order of single crystal electrodes upon immersion into the electrochemical environment. The variations in the SHG response from the electrode upon rotation about the surface normal reflect the average symmetry of the first few atomic layers of the metal surface. SHG rotational anisotropy has been applied both in UHV [21,22], and in electrochemical environments [23–26]. Symmetry and chemisorption information can also be obtained by monitoring the changes in the SHG signal at a fixed azimuthal angle as a function of electrode potential [27–30]. In this paper we employ both types of SHG measurements to study chemisorption at the well-ordered Pt(111) surface.

The second harmonic nonlinear optical response of a system to an incident light field at frequency ω is the result of the nonlinear polarization $\boldsymbol{P}_0^{(2)}(2\omega)$ that is induced in the material. This induced nonlinear polarization is related to the incident electric field $\boldsymbol{E}(\omega)$ by the nonlinear susceptibility $\chi^{(2)}$:

$$\boldsymbol{P}_0^{(2)}(2\omega) \propto \chi^{(2)}: \boldsymbol{E}(\omega)\boldsymbol{E}(\omega) \tag{1}$$

At an interface, there is a contribution to $\chi^{(2)}$ from the surface, $\chi_S^{(2)}$, and a contribution from the adjacent bulk media, $\chi_B^{(2)}$:

$$\chi^{(2)} = \chi_B^{(2)} + \chi_S^{(2)} \tag{2}$$

The relations between the observed SHG signal intensity $I(2\omega)$ and $\chi^{(2)}$ have been described by Sipe [31] for the (111), (110) and (100) surfaces of face-centered cubic metals. In centrosymmetric media, the SHG process is electric dipole forbidden and $\chi_B^{(2)}$ results only from the higher order magnetic dipole and electric quadrupole contributions. For a metal–solution interface, the higher order contributions from the bulk solution are expected to be negligible, but the higher order bulk contributions to $\chi^{(2)}$ from the metal can be significant.

In contrast, the surface contribution to the nonlinear susceptibility $\chi_S^{(2)}$ is allowed at the interface of two centrosymmetric media, and therefore is the sum of electric dipole and higher order multipole (nonlocal) contributions. In electrochemical systems, the potential dependence of the SHG signal has been used to obtain estimates of the relative bulk and surface contributions to $\chi^{(2)}$, since only $\chi_S^{(2)}$ should vary with changes in the surface electric fields. For platinum electrodes, the elements of $\chi_S^{(2)}$ from the metal–solution interface have been found to be usually comparable to or larger in magnitude than the corresponding elements of $\chi_B^{(2)}$ [30].

In the presence of an adsorbate, the surface nonlinear susceptibility $\chi_S^{(2)}$ is modified by the presence of the chemisorbed species to a new value χ_S' [32,33]:

$$\chi_S'^{(2)} = \chi_S^{(2)} + \chi_A^{(2)} + \Delta\chi_I^{(2)} \tag{3}$$

where $\chi_A^{(2)}$ is the inherent nonlinear susceptibility of the adsorbate independent of the surface and $\Delta\chi_I^{(2)}$ is the change in nonlinear susceptibility of the surface and adsorbate due to any interactions. If the nonlinear susceptibility of the metal surface $\chi_S^{(2)}$ is much larger than $\chi_A^{(2)}$, the only changes that will be observed upon adsorption will be due to $\Delta\chi_I^{(2)}$. Studies which use these changes in $\chi_S'^{(2)}$ to obtain information on chemisorption at electrode surfaces are called nonresonant SHG studies, and have been employed at a number of metal electrode surfaces [25–30]. In other cases it is possible to choose an adsorbate and a wavelength for which $\chi_A^{(2)}$ is the dominant contribution to $\chi_S'^{(2)}$; these studies are called resonant SHG experiments, and have been used to obtain the average molecular orientation of an adsorbate at both electrochemical [34] and nonconducting surfaces [33,35].

In this paper we utilize in situ nonresonant SHG measurements as a function of azimuthal angle and electrode potential to monitor the chemisorption processes at a flame-annealed well-ordered Pt(111) electrode. An ordered monolayer of iodine is adsorbed onto the flame-annealed single crystal in an argon atmosphere; in situ

SHG measurements confirm that the chemisorbed iodine reduces the average surface symmetry of the electrode, yet maintains the crystal surface order upon transfer to an electrochemical environment. The replacement of the iodine monolayer with carbon monoxide and the subsequent oxidation of the surface CO lead to a surface which exhibits the clean, well-ordered Pt(111) voltammetry in perchloric acid solutions. The potential dependence of the SHG signal from the surface is presented in detail and compared with that from Pt(100) and polycrystalline Pt electrodes; for the well-ordered Pt(111) surface chemisorbed species are observed at all potentials. In particular, an ordered monolayer of a hydrogen or hydronium ion species is observed throughout the double layer and hydrogen regions, and two types of adsorbed oxide/hydroxide monolayers are observed at potentials positive of the double layer region.

EXPERIMENTAL

The SHG signal measured in these experiments was created on the electrode surface from the 2 ps pulses of light at 605 nm generated by a 4 MHz dye laser (Coherent Model 702CD) synchronously pumped by a mode-locked Nd : YAG laser (Coherent Model Antares 76S). Each pulse had approximately 35 nJ of laser energy and was focused to a 0.1 mm spot on the surface. The SHG experiments were performed at an incident angle of 60° with respect to the surface normal and the anisotropic SHG response of the electrode was obtained by rotating the crystal about this axis. The azimuthal angle was defined as the angle between the plane of incidence for the fundamental beam and the $[2\bar{1}\bar{1}]$ axis of the Pt(111) surface as determined by Laue back-scattering. The SHG signal was obtained with a photon counting system and was normalized by a separate reference channel. The reference channel consisted of an ADP doubling crystal, filters and a photodiode which generated an output voltage that reflected any variations in laser power or pulse width over the course of the experiment. The normalized SHG signal consisted of the number of counts obtained in one second of integration time divided by the reference channel voltage (which was set to an average of one volt), and is expressed in counts s^{-1}. The polarizations of the fundamental and second harmonic beams were set to either s-polarization (perpendicular to the plane of incidence) or p-polarization (parallel to the plane of incidence) with Glan Laser polarizers (Special Optics) that had extinction ratios of 10^{-5}. Experiments with a second Glan Laser polarizer inserted into the second harmonic or fundamental beam demonstrated that there was no polarization leakage in the crossed polarization measurements.

The electrode in the experiments was a 6 mm diameter polished Pt(111) crystal obtained from Aremco. Laue diffraction measurements revealed that the crystal was polished to within a degree of the (111) surface. Prior to the immersion of the electrode the Pt crystal was heated to 800 °C in a hydrogen flame and then cooled in an argon/iodine vapor stream in a manner which has been found to form a $\sqrt{7} \times \sqrt{7}$ chemisorbed iodine overlayer [36]. The electrode was then mounted on a glass

rod, sealed around the edge with teflon tape, and then immersed into a two window spectroelectrochemical cell [30]. The cell contained approximately 100 ml of a 0.1 M $HClO_4$ (doubly-distilled from Vycor GFS Chemicals) solution prepared from water that was Millipore-filtered and then doubly distilled. The electrode potential was controlled by a Princeton Applied Research 173/175 potentiostat; all potentials are reported versus a Ag/AgCl(sat'd NaCl) reference that was isolated from the main solution. In addition to the SHG anisotropy measurements, the potential dependence of the SHG signal at a fixed azimuthal angle was obtained simultaneously with the cyclic voltammograms (CVs) at a scan rate of 20 mV s^{-1}; both measurements were captured digitally and stored on a computer. The potential dependent SHG signal is expressed in counts s^{-1} and is normalized to the same scale as the SHG signal from the anisotropy measurements.

RESULTS AND DISCUSSION

Iodine monolayer formation

The SHG anisotropy measurements $I_{p,s}(2\omega)$ and $I_{s,p}(2\omega)$ from the iodine-coated Pt(111) surface at an electrode potential of +0.200 V are shown in Fig. 1, where the

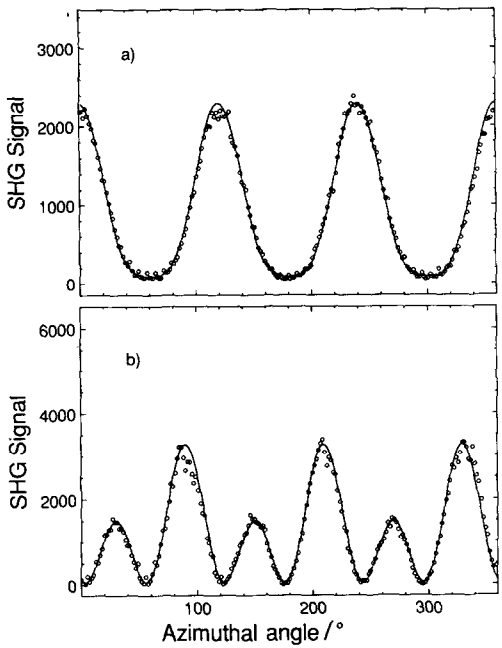

Fig. 1. The SHG signals (a) $I_{s,p}(2\omega)$ and (b) $I_{p,s}(2\omega)$ as a function of azimuthal angle for a flame-annealed Pt(111) electrode with an adsorbed monolayer of atomic iodine in 0.1 M $HClO_4$ at an electrode potential of +0.200 V, where $I_{input,output}(2\omega)$ refer to the input and output beam polarizations. The solid lines are fits to eqns. (5) and (6′) for $I_{s,p}(2\omega)$ and $I_{p,s}(2\omega)$ respectively.

subscripts of the SHG signal $I_{\text{input,output}}(2\omega)$ refer to the polarization of the incident (input) and second harmonic (output) light fields [s = s-polarized light and p = p-polarized light]. The ϕ-dependence of the SHG response reflects the average symmetry of the bulk, surface, and adsorbate contributions to the nonlinear susceptibility. For a bare Pt(111) surface, the azimuthal dependence of the SHG signal can be written as [31]:

$$I_{\text{p,p}}(2\omega) = |\, a_{\text{p,p}} + c_{\text{p,p}} \cos(3\phi) \,|^2 \tag{4}$$

$$I_{\text{s,p}}(2\omega) = |\, a_{\text{s,p}} + c_{\text{s,p}} \cos(3\phi) \,|^2 \tag{5}$$

$$I_{\text{p,s}}(2\omega) = |\, b_{\text{p,s}} \sin(3\phi) \,|^2 \tag{6}$$

$$I_{\text{s,s}}(2\omega) = |\, b_{\text{s,s}} \sin(3\phi) \,|^2 \tag{7}$$

where the complex constants $a_{\text{in,out}}$, $b_{\text{in,out}}$ and $c_{\text{in,out}}$ are combinations of bulk and surface contributions to $\chi^{(2)}$ multiplied by the incident laser power and the Fresnel coefficients at the incident and second harmonic wavelengths. The surface and bulk contributions have been described by Sipe [31], and can also be found in ref. 27. (Note: our notation differs slightly from that of Sipe in that the incident laser power and second harmonic Fresnel coefficient are incorporated into the complex constants $a_{\text{in,out}}$, $b_{\text{in,out}}$ and $c_{\text{in,out}}$. For example, $a_{\text{s,p}} = a_{\perp,\parallel} I_{\text{s}} A_{\text{p}}$ from eqn. 32 of ref. 31.) The surface contribution to the nonlinear susceptibility, $\chi_{\text{S}}^{(2)}$, has been shown to reflect the symmetry of the first few layers of surface atoms [21]. The first three atomic layers of a bare Pt(111) surface are depicted in Fig. 2a, with the $[2\bar{1}\bar{1}]$ directions given by solid lines. These three monolayers have an overall symmetry of C_{3v}. For a surface with C_{3v} symmetry there will be only 4 independent nonzero tensor elements of $\chi_{\text{S}}^{(2)}$: χ_{ZZZ}, $\chi_{ZXX} = \chi_{ZYY}$, $\chi_{XXZ} = \chi_{XZX} = \chi_{YYZ} = \chi_{YZY}$, and $\chi_{XXX} = -\chi_{YXY} = -\chi_{YYX} = -\chi_{XYY}$ [31,32]. These allowed surface nonlinear susceptibility tensor elements are contained in the a, b and c constants. For example, the χ_{XXX} surface susceptibility tensor element will contribute to $c_{\text{s,p}}$ and $b_{\text{p,s}}$. Table 1 lists which surface tensor elements are associated with which constants for the C_{3v} surface; full relations for other surface symmetries can be found elsewhere [32].

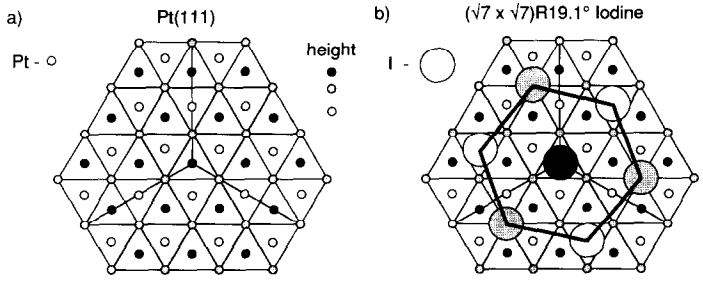

Fig. 2. Diagram of the first three monolayers of a Pt(111) surface: (a) bare surface (C_{3v} symmetry) and (b) surface with a $(\sqrt{7} \times \sqrt{7})R19.1°$ adsorbed iodine monolayer (C_3 symmetry).

TABLE 1

Relations between the nonlinear surface susceptibility tensor elements and the SHG optical constants for the Pt(111) electrode surface

SHG constant [a]	C_{3v} symmetry	C_3 symmetry [b]
$a_{p,p}$	χ_{ZXX}, χ_{XXZ}, χ_{ZZZ}	χ_{ZXX}, χ_{XXZ}, χ_{ZZZ}
$b_{p,p}$	–	χ_{YYY}
$c_{p,p}$	χ_{XXX}	χ_{XXX}
$a_{s,p}$	χ_{ZXX}	χ_{ZXX}
$b_{s,p}$	–	χ_{YYY}
$c_{s,p}$	χ_{XXX}	χ_{XXX}
$a_{p,s}$	–	χ_{XYZ}
$b_{p,s}$	χ_{XXX}	χ_{XXX}
$c_{p,s}$	–	χ_{YYY}
$a_{s,s}$	–	–
$b_{s,s}$	χ_{XXX}	χ_{XXX}
$c_{s,s}$	–	χ_{YYY}

[a] These constants are defined in the text.

[b] These are the surface tensor elements that are allowed when the average surface symmetry is reduced from C_{3v} to C_3 by the presence of an adsorbate.

Using eqn. (5), the angular dependence of $I_{s,p}(2\omega)$ depicted in Fig. 1a can be fit with the ratio $|a_{s,p}|/|c_{s,p}| = 1.14$ and a phase difference between $a_{s,p}$ and $c_{s,p}$ of $\Delta\gamma = 22°$ (since the coefficients a, b and c are complex we must define both a relative magnitude and phase).

In contrast, the angular dependence observed for $I_{p,s}(2\omega)$ in Fig. 1b is an alternating sixfold pattern which *cannot* be fit by the theory of SHG from a C_{3v} surface (eqn. 6, which predicts a uniform sixfold pattern). Instead, the anisotropic response observed from the surface implies that there must be a constant term $a_{p,s}$ contributing to $I_{p,s}(2\omega)$:

$$I_{p,s}(2\omega) = |a_{p,s} + b_{p,s}\sin(3\phi)|^2 \qquad (6')$$

The angular dependence of $I_{p,s}$ can be fit by Eqn. (6′) with a ratio $|a_{p,s}|/|b_{p,s}| = 0.25$ and a phase difference between $a_{p,s}$ and $b_{p,s}$ of $\Delta\gamma = 240°$. The presence of an adsorbate can alter the symmetry of the surface and change the number of tensor elements allowed for $\chi_S^{(2)}$. This in turn will lead to a different azimuthal angle dependence for the SHG signal. For example, iodine is expected to adsorb onto a flame-annealed Pt(111) electrode in a $(\sqrt{7} \times \sqrt{7})R19.1°$ overlayer structure [9,36] (Fig. 2b). The iodine atoms in this structure sit in three different adsorption sites: one on top of a platinum atom (black) and two in nonequivalent surface hollows (white and shaded). This overlayer has C_{3v} symmetry, but with its mirror plane axis rotated by 19.1° relative to the $[2\bar{1}\bar{1}]$ surface axis. If we add the contributions of $\chi_A^{(2)}$ and $\Delta\chi_I^{(2)}$ to $\chi_S^{(2)}$, the resultant surface symmetry is reduced from C_{3v} to C_3. For a C_3 surface two additional tensor elements can be nonzero: $\chi_{XYZ} = \chi_{XZY} = -\chi_{YXZ} = -\chi_{YZX}$ and $\chi_{YYY} = -\chi_{YXX} = -\chi_{XXY} = -\chi_{XYX}$ [32]. For the SHG signal $I_{p,s}(2\omega)$, these two new elements can result in the possible nonzero complex

constants $a_{p,s}$ and $c_{p,s}$ respectively. Since the observed $I_{p,s}(2\omega)$ anisotropy can be described by eqn. (6′), the presence of the iodine monolayer has reduced the average surface symmetry and created a nonzero χ_{XYZ} nonlinear surface susceptibility tensor element. No evidence for a nonzero χ_{YYY} surface tensor element was found. This means that either $|\chi_{YYY}|$ is inherently small, or there is an interference between the resonant and non-resonant surface contributions to χ_{YYY}. Table 1 has a complete list of the possible complex constants which could appear when the average symmetry of the surface is reduced to C_3. Note that $I_{s,p}(2\omega)$ is unaffected by the presence of a nonzero χ_{XYZ}, so that eqn. (5) remains valid.

The interpretation of the average surface symmetry for an electrode with an adsorbed overlayer is complicated by the fact that different domain structures can form on the surface. For example, the $(\sqrt{7} \times \sqrt{7})R19.1°$ iodine monolayer can adsorb in two possible domains on the C_{3v} Pt(111) surface. One domain is shown in Fig. 2b. The other domain can be generated by reflecting the iodine monolayer about the $[2\bar{1}\bar{1}]$ symmetry axis. If these two domains are equally populated, then the average surface symmetry returns again to C_{3v}, and the average tensor element $\langle\chi_{XYZ}\rangle$ becomes zero for the surface. The fact that the SHG response can be fit by eqn. (6′) means that there must be an unequal distribution of domains on this flame-annealed electrode which lead to a reduction of the average surface symmetry from C_{3v} to C_3. In a recent SHG study of gold single crystal electrodes, Friedrich et al. [25] also observed the presence of unequal domain distributions on the surface with the anisotropic SHG response.

The full iodine monolayer is stable over a wide potential range on the Pt(111) surface, and the constants $|a_{p,s}|$, $|b_{p,s}|$ and $\Delta\gamma$ can be measured as a function of potential. These constants can be determined either by fitting the entire rotational anisotropy function at each potential, or by measuring the SHG signal simultaneously with the voltammetry during a CV at a number of fixed azimuthal angles. For example, by measuring the potential dependence of $I_{p,s}(2\omega)$ at $\phi = 0°$, $30°$, and $-30°$ we can reconstruct the potential dependence of the three constants by using the following equations:

$$|a_{p,s}|^2 = I_{p,s}(2\omega, \phi = 0°) \tag{8}$$

$$|b_{p,s}|^2 = 0.5\{I_{p,s}(2\omega, \phi = -30°) + I_{p,s}(2\omega, \phi = 30°)\} - |a_{p,s}|^2 \tag{9}$$

$$\cos\Delta\gamma = 0.25\{I_{p,s}(2\omega, \phi = 30°) - I_{p,s}(2\omega, \phi = -30°)\}/\{|a_{p,s}||b_{p,s}|\} \tag{10}$$

The magnitude of $|a_{p,s}|$ and $|b_{p,s}|$ for the iodine monolayer that was obtained as the potential was cycled between -0.175 V and -0.600 V is plotted in Fig. 3 ($\Delta\gamma$ was also calculated but is omitted for the sake of brevity). The constant $|a_{p,s}|$ is found to vary linearly with potential, while $|b_{p,s}|$ is relatively potential independent. Since the surface coverage of the iodine is constant in this potential range, the variation in $a_{p,s}$ (and therefore in the surface tensor element χ_{XYZ}) with potential must be attributed to alterations in the surface/chemisorbate electronic structure induced by the static dc electric fields. These changes can either occur via a

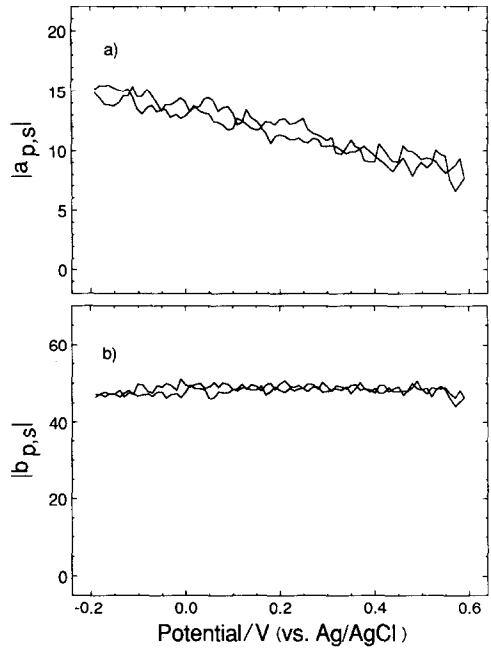

Fig. 3. Potential dependence of the constants $a_{p,s}$ (a) and $b_{p,s}$ (b) from a well-ordered Pt(111) surface with a full adsorbed iodine monolayer as calculated from the potential dependence of $I_{p,s}(2\omega)$ at azimuthal angles of 0, −30, and 30° (eqns. 8 and 9).

hyperpolarizability effect [28], or through changes in the chemisorbate-surface interactions with the fields. In contrast, the $|b_{p,s}|$ term (and therefore the surface tensor element χ_{XXX}) is less sensitive to the static dc fields. The presence of these dc field effects implies that the SHG signal will not always be correlated with the faradaic currents.

CO monolayer formation and removal

Electrochemical oxidation of the iodine monolayer to iodate leads to a disordered surface. In order to avoid this disordering, Zurawski et al. replaced the adsorbed iodine with a monolayer of CO [14]. This CO monolayer can be electrochemically oxidized to CO_2 without disordering the surface. Figures 4a and 4b plot the anisotropic response of $I_{s,p}(2\omega)$ and $I_{p,s}(2\omega)$ from the Pt(111) electrode at a potential of +0.200 V after the iodine monolayer has been replaced with carbon monoxide from a saturated CO solution at an electrode potential of +0.050 V. The replacement reaction in saturated CO solution at this electrode potential leads to a highly packed CO monolayer with a surface density of 0.62–0.68 CO molecules per Pt surface atom [14,20]. A marked change in the angular dependence of $I_{s,p}(2\omega)$ and the continued presence of the alternating sixfold pattern for the $I_{p,s}(2\omega)$ anisotropic response are observed. These measurements, as well as measurements on partial CO

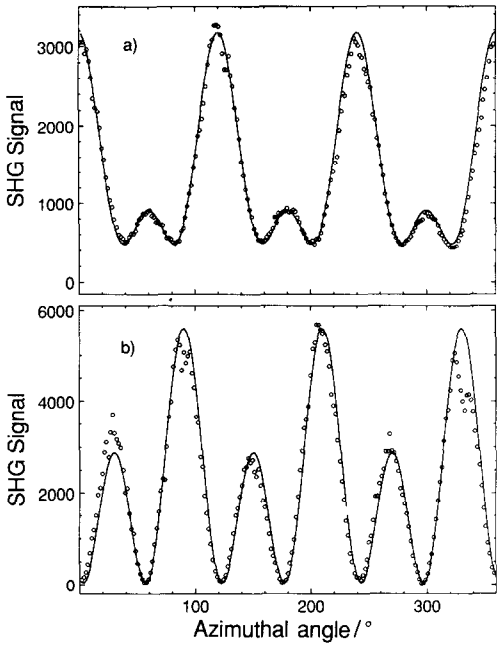

Fig. 4. The SHG signals (a) $I_{s,p}(2\omega)$ and (b) $I_{p,s}(2\omega)$ as a function of azimuthal angle for a flame-annealed Pt(111) electrode with a highly packed CO monolayer in 0.1 M $HClO_4$ at an electrode potential of +0.200 V. The solid lines are fits to eqns. (5) and (6′) for $I_{s,p}(2\omega)$ and $I_{p,s}(2\omega)$ respectively.

monolayers, can again be accounted for with a reduced average surface symmetry of C_3 (or less), and are discussed in detail elsewhere [26,37].

The highly packed CO monolayer is oxidized electrochemically to CO_2 by scanning positively at a rate of 50 mV s^{-1}. Figure 5a plots the CV obtained during this oxidation; integration of the current peak at +0.540 V leads to a surface charge density for the monolayer of 305 μC cm^{-2}, which is in good agreement with the results of other authors [14,20]. Continued cycling between −0.220 V and 0.830 V results in the steady state CV shown in Fig. 5b. This CV is indicative of the highly ordered Pt(111) surface obtained originally by Clavilier [1], with the following features: (i) a sharp, reversible pair of "butterfly" peaks at 0.510 V, (ii) a broad, reversible pair of peaks just negative of the butterfly peaks at 0.480 V, (iii) an irreversible oxide peak at 0.780 V and (iv) a pair of reversible hydrogen "waves" at 0.0 V. The presence of these four features has been used by previous authors as an indication of a well-ordered Pt(111) surface [1,12,14].

Hydrogen and hydronium ion adsorption

The potential dependence of the SHG signal $I_{p,p}(2\omega)$ at an azimuthal angle of $\phi = 30°$ for a well-ordered Pt(111) surface during a CV is shown in Fig. 6a. A pronounced increase in the SHG signal is observed at potentials below +0.480 V,

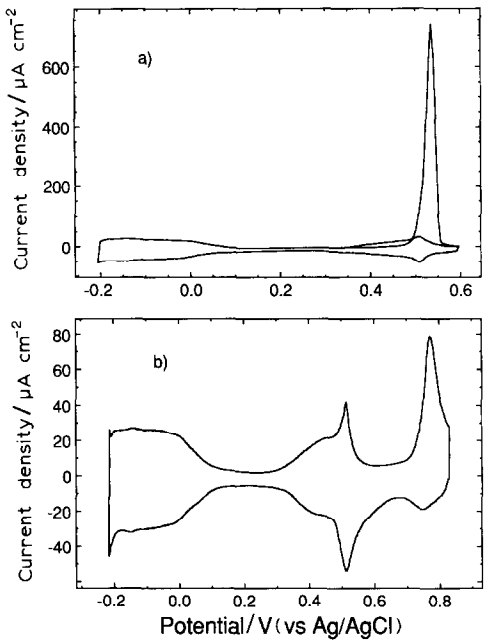

Fig. 5. Cyclic voltammetry obtained from the Pt(111) electrode (a) during oxidation of the full CO monolayer, and (b) immediately following removal of the CO and formation of a well-ordered Pt(111) surface. Scan rate: 50 mV s^{-1}.

the potential at which the broad anomalous wave is observed on this surface. Clavilier has attributed this wave to the deposition of a strongly adsorbed hydrogen species [1], and Ross has proposed that this hump is a capacitive peak due to the ordered adsorption of hydronium ions [13]. For comparison, the potential dependence of the $I_{p,p}(2\omega)$ SHG signal for a Pt(100) surface and a polycrystalline Pt surface are shown in Figs. 6b and c respectively. On both of these surfaces an increase in the SHG signal is observed at potentials at which current peaks that are associated with the adsorption of hydrogen occur.

An increase in the SHG signal from a Pt(111) surface upon the chemisorption of hydrogen has also been observed previously in UHV [22]. In that study the SHG signal was found to be inversely correlated to changes in the surface work function upon chemisorption for a number of adsorbates. The chemisorption of hydrogen decreased the work function of the Pt(111) surface by 0.23 eV, and led to an increased surface free electron density at the surface. The nonresonant nonlinear optical susceptibility of a metal surface is dominated by the nonlinear response of the free electrons, so that an increase in surface free electron density results in an increase in the surface SHG signal. An additional resonant enhancement of the SHG signal may occur upon the adsorption of hydrogen onto the Pt(111) surface. Photoemission experiments on Pt(111) have shown dramatic changes in the Pt *d*-band states 4 eV below the Fermi level upon hydrogen chemisorption [38].

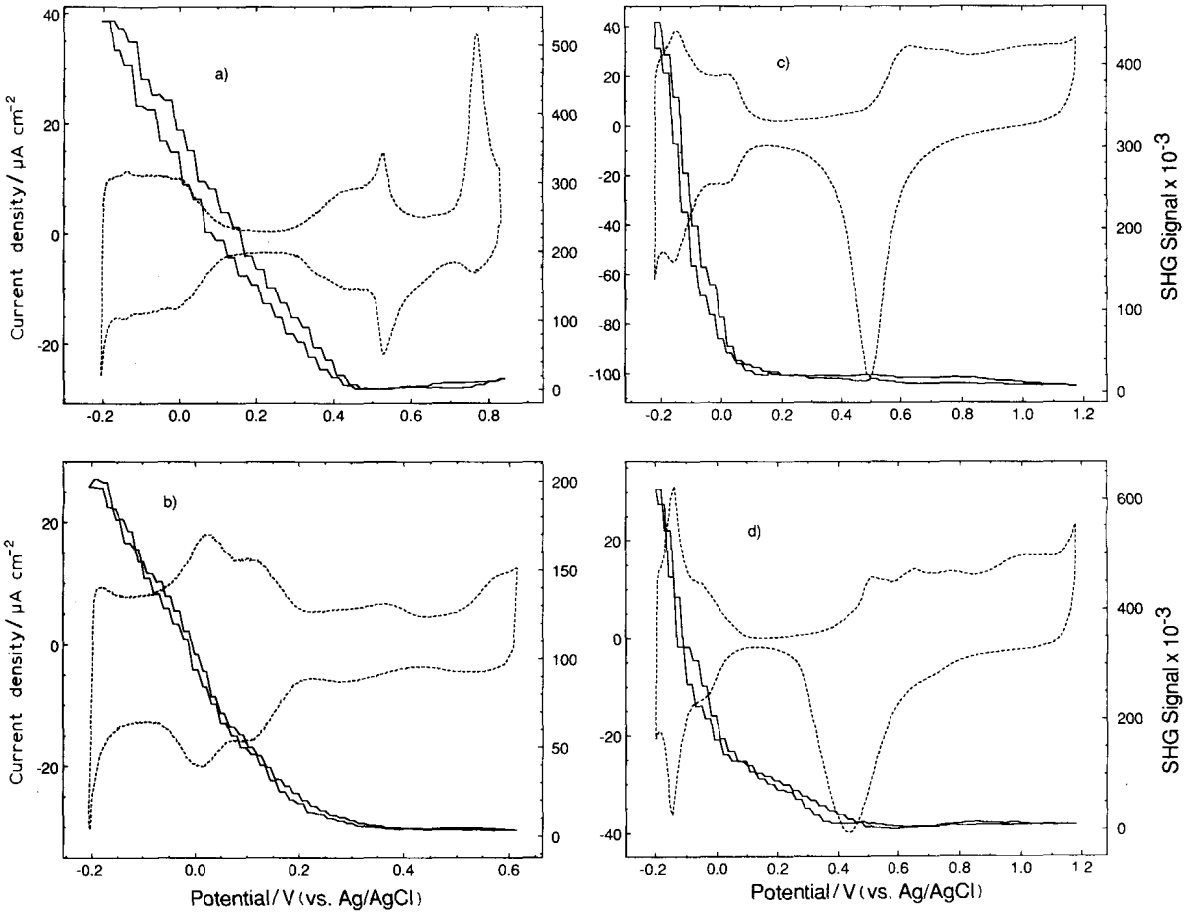

Fig. 6. Cyclic voltammetry and potential dependence of the $I_{p,p}(2\omega)$ SHG signal from: (a) a well-ordered Pt(111) surface oriented with an azimuthal angle of 0°, (b) a well-ordered Pt(100) surface (c) a polycrystalline Pt surface and (d) a disordered Pt(111) surface oriented with an azimuthal angle of 0° after several cycles. All electrochemistry was performed in 0.1 M perchloric acid. Scan rate: 20 mV s^{-1}.

Interband transitions from these states to unoccupied levels above the Fermi level could resonantly enhance the SHG signal at the near UV wavelength employed in our studies [22].

It is tempting on the basis of the above evidence to relate the rise in the SHG signal on the Pt(111) surface to the presence of adsorbed hydrogen at all potentials below +0.480 V on the well-ordered Pt(111) surface. However, one must remember that the nonresonant SHG signal is an indirect measurement of chemisorption, and cannot definitively identify the chemisorbed species. The chemisorption of the hydrogen in an adsorbed H_3O^+ species that perturbs the platinum surface wavefunctions strongly could also conceivably lead to the increase in the SHG signal. In fact, although the potential dependence of the $I_{p,p}(2\omega)$ SHG signal on all three platinum surfaces (Pt(111), Pt(100) and polycrystalline) is found to be very sensitive to the adsorption of hydrogen, the potential dependence of the $I_{p,p}(2\omega)$ SHG signal for the well-ordered Pt(111) surface in the double layer region does not correlate with the currents observed from the electrode. A monotonic increase in $I_{p,p}(2\omega)$ is observed at all potentials below +0.480 V. The lack of correlation of the SHG signal to the currents on this single crystal surface suggests that there are changes with potential in the electronic structure of the surface-hydrogen (or surface-hydronium ion) interaction similar to those observed in the case of an iodine monolayer (as described in section A).

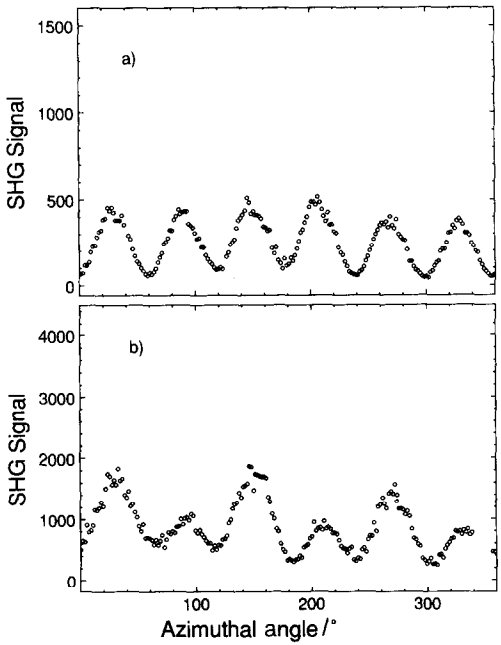

Fig. 7. The SHG signal $I_{p,s}(2\omega)$ as a function of azimuthal angle for the well-ordered Pt(111) electrode in 0.1 M $HClO_4$ at a potential of (a) +0.200 V, and (b) −0.175 V.

The adsorption of hydrogen species on these surfaces can be examined in more detail with the potential dependence of the $I_{p,s}(2\omega)$ SHG signal. Figure 7a plots the azimuthal dependence of $I_{p,s}(2\omega)$ at a potential of +0.200 V. In comparison with the $I_{p,s}(2\omega)$ from the surface with an iodine monolayer, it is much closer to the symmetric sixfold pattern predicted from C_{3v} symmetry (eqn. 6). However, there is a small amount of an $a_{p,s}$ contribution that becomes more pronounced as the potential is scanned into the hydrogen region; for example, the SHG anisotropy observed at −0.175 V (Fig. 7b) exhibits a pronounced alternating sixfold pattern that arises from the $a_{p,s}$ term in eqn. (6′). As in the case of iodine, a nonzero $a_{p,s}$ implies that the presence of the adsorbate has created a nonzero $\langle \chi_{XYZ} \rangle$ from the surface, and is evidence for the ordered adsorption of species onto the electrode surface. Additional evidence for the formation of an ordered adsorbate monolayer on both Pt(111) and Pt(100) surfaces has been found in the presence of bisulfate anions [37].

A more complete picture of the potential dependence of $a_{p,s}$ can be obtained by measuring $I_{p,s}(2\omega)$ at the fixed azimuthal angle of 0° during a CV (Fig. 8a). This SHG signal is directly proportional to $|a_{p,s}|^2$ (eqn. 8). The potential dependence of $|a_{p,s}|$ is found to be similar to the $I_{p,p}(2\omega)$ SHG signal: near zero at all potentials

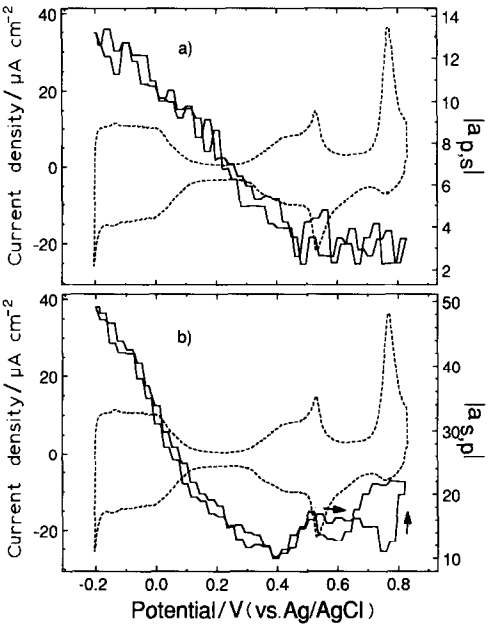

Fig. 8. Cyclic voltammetry and potential dependence of (a) $|a_{p,s}|$ (obtained from $I_{p,s}(2\omega)$ at an azimuthal angle of 0°) and (b) $|a_{s,p}|$ (obtained from $I_{s,p}(2\omega)$ at an azimuthal angle of 30°) from a well-ordered Pt(111) surface in 0.1 M perchloric acid. Scan rate: 20 mV s^{-1}. The arrows on the SHG signal refer to the response obtained during the positive sweep of the CV.

above +0.480 V and monotonically increasing at all potentials below +0.480 V. The presence of $a_{p,s}$ demonstrates the presence of an ordered adsorption with C_3 symmetry or less throughout this potential range, and the monotonicity of the SHG signal as a function of potential suggests a continuous change in the electronic structure of the surface throughout this region. These changes could occur from the perturbation of the surface by an adsorbed H_3O^+ species as it converts to an adsorbed hydrogen species, and therefore does not necessarily have to correlate with the voltammetry.

In contrast to the potential dependence of $a_{p,s}$, the constant $b_{p,s}$ (which was independent of potential for the iodine monolayer) exhibits a complex potential dependence for the well-ordered Pt(111) electrode. As in the case of iodine, the potential dependence of the constant $|b_{p,s}|$ during a CV can be calculated from $|a_{p,s}|$ and the $I_{p,s}(2\omega)$ signal at the azimuthal angles of -30, and $30°$ (Figs. 9a and b). The potential dependence of $|b_{p,s}|$ calculated from these two curves is shown in Fig. 9c, and reaches a mininum on both the negative and positive sweeps just negative of the butterfly peaks. The constant $|b_{p,s}|$ rises quickly once during the broad peak at +0.450 V and a second time during the deposition of hydrogen at 0.000 V, demonstrating that the surface tensor element $\langle \chi_{XXX} \rangle$ is sensitive to the various hydrogen/hydronium ion structures which exist on the surface. Variations are also observed in the constant $|a_{s,p}|$ through the surface tensor element $\langle \chi_{ZXX} \rangle$ on the well-ordered Pt(111) surface (Fig. 8b).

OH and oxide formation on the Pt(111) electrode

At potentials positive of the butterfly peaks the Pt(111) surface undergoes a series of oxidative processes, and although $I_{p,p}(2\omega)$ is small, it of course does not mean that there is an absence of chemisorption in this region. Not all chemisorbates will increase the SHG signal from the platinum surface; for example, the adsorption of oxygen onto metal surfaces in UHV increases the work function of the surface and thus decreases the SHG signal [22]. In an electrochemical environment, the adsorption of an oxide species onto a polycrystalline platinum electrode has been found to depress $I_{p,p}(2\omega)$ as compared to the bare surface [30]. A similar decrease is observed on the Pt(111) surface at all potentials positive of the butterfly peaks (Fig. 6a).

In addition to the loss of the $I_{p,p}(2\omega)$ SHG signal, the potential dependence of $|b_{p,s}|$ and $I_{p,s}(2\omega)$ at $-30°$ and $30°$ (Fig. 9) can be used to monitor the formation of surface oxide monolayers. In Fig. 9c, $|b_{p,s}|$ reaches a constant level after the butterfly peaks on the positive scan. Previous authors have suggested that an OH species resides on the surface in this region [11]. After the first oxide peak at +0.770 V, $|b_{p,s}|$ increases to a second level. The formation of this oxide is an irreversible process, and on the return sweep $|b_{p,s}|$ remains at this second level until approximately +0.650 V, when it returns to the level of the OH species at about +0.570 V, and then to a minimum after the butterfly peaks.

A closer examination of Figs. 9a and b reveals that the $I_{p,s}(2\omega)$ ($\phi = -30°$) SHG signal is sensitive to both the OH adsorption and oxide formation, whereas the $I_{p,s}(2\omega)$ ($\phi = 30°$) SHG signal changes primarily during the first oxide peak. Since

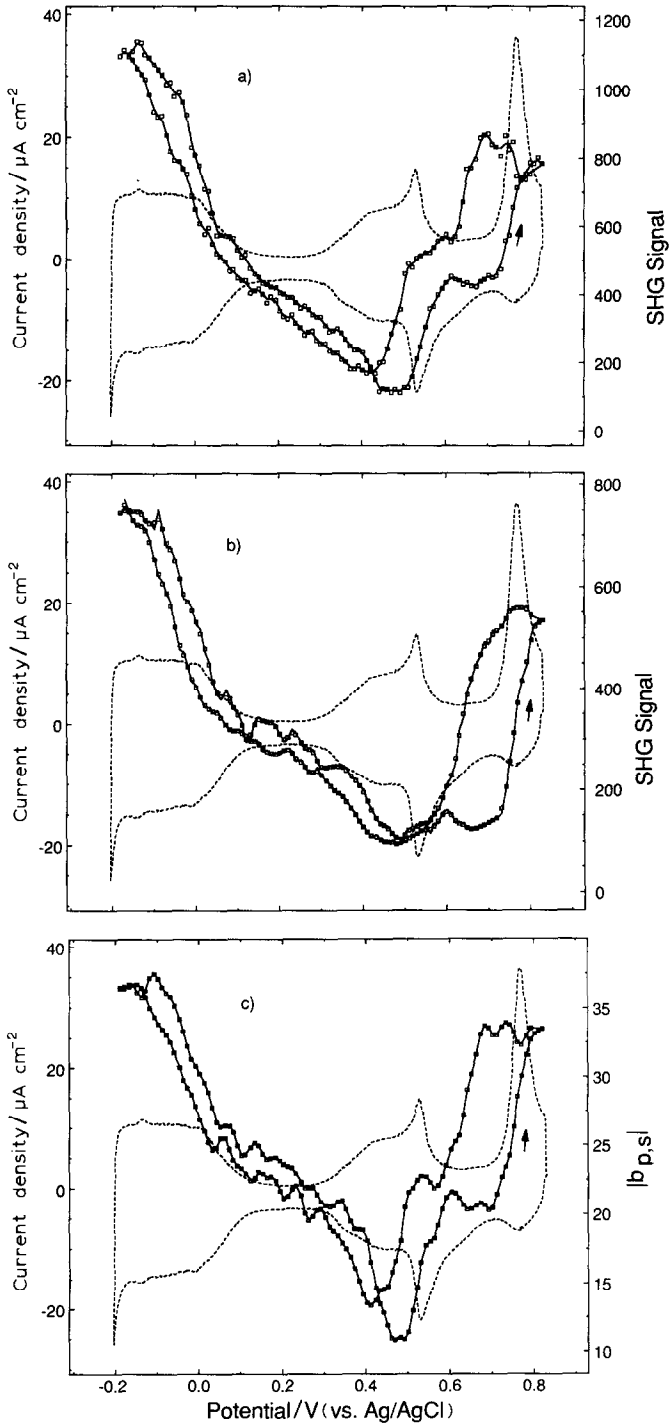
a)
b)
c)
Current density / μA cm^{-2}
SHG Signal
$|b_{p,s}|$
Potential / V (vs. Ag/AgCl)
40
20
0
-20
1200
1000
800
600
400
200
0
35
30
25
15
10
-0.2
0.0
0.2
0.4
0.6
0.8

$|a_{p,s}|$ is virtually zero in this potential region, the differences in the $I_{p,s}(2\omega)$ SHG signal in Figs. 9a and b imply additional changes in the functional form of the SHG anisotropy from the surface (eqn. 6′). For example, the presence of surface and overlayer contributions to $\langle \chi_{XXX} \rangle$ with a ϕ dependence that is 90° out of phase could lead to the $I_{p,s}(2\omega)$ signals observed in Fig. 9. Similar ϕ dependence differences between a substrate and an overlayer have been observed in the underpotential deposition of Cd on Ag [24]. A full symmetry analysis of $I_{p,s}(2\omega)$ in the oxide regions will be presented elsewhere [37]. From the potential dependence of the $I_{p,s}(2\omega)$ SHG signal in Fig. 9, it is clear that all of the voltammetry on the well-ordered Pt(111) surface positive of the butterfly peaks can be attributed to changes in the surface oxide structure, and that all of these changes can be followed by the nonresonant SHG signal.

Further oxide formation and disordering of the surface

If the window of the CV from the well-ordered Pt(111) surface is expanded to 0.900 V, a surface oxide is formed at higher potentials and changes are observed in the hydrogen region of the CV. It has been found that cycling the potential to these more positive values disorders the surface [1,12] and creates a new hydrogen peak at −0.140 V (this peak was originally observed by Will [3]). The disordering also affects the $I_{p,p}(2\omega)$ SHG signal with a large increase observed in conjunction with the new hydrogen peak and a gradual decrease of the SHG signal in the double layer region (Fig. 6d). The change in the potential dependence of $I_{p,p}(2\omega)$ from the Pt(111) surface upon disordering confirms that the chemisorbed structure responsible for the anomalous voltammetry is present only on the well-ordered surface, and that a different type of adsorbed hydrogen is present on the disordered surface as compared to the well-ordered electrode. Upon cycling to very positive potentials in either perchloric acid or sulfuric acid [37], the ordered adsorbate structure in the double layer region is gradually destroyed on the single crystal surface.

CONCLUSIONS

In summary, in this paper we have demonstrated that the surface structure of a well-ordered Pt(111) electrode is maintained throughout the series of electrochemical chemisorption and oxidation steps required during its formation. The formation of an iodine monolayer and a highly packed CO monolayer is easily observed with the SHG anisotropy measurements. Additional contributions to the surface SHG signal are observed with these monolayers and can be attributed to the additional surface contributions to the nonlinear susceptibility that appear upon reduction of

Fig. 9. Cyclic voltammetry and potential dependence of (a) $I_{p,s}(2\omega)$ at an azimuthal angle of −30°, (b) $I_{p,s}(2\omega)$ at an azimuthal angle of +30°, and (c) $|b_{p,s}|$ (obtained from eqn. 9) from a well-ordered Pt(111) surface in 0.1 M perchloric acid. Scan rate: 20 mV s^{-1}. The arrows on the SHG signal refer to the response obtained during the positive sweep of the CV.

the average surface symmetry. In the absence of iodine or CO adsorption, the order of the Pt(111) surface is preserved and the presence of an adsorbed species with an $I_{p,p}(2\omega)$ SHG response similar to adsorbed hydrogen on Pt(100) and polycrystalline surfaces is detected at potentials negative of +0.450 V. The $I_{p,s}(2\omega)$ response from the surface verifies the presence of an ordered adsorbate monolayer at these potentials, and also identifies additional adsorbate species in the oxide, hydrogen and butterfly regions. Due to the indirect nature of these SHG measurements, the identity of the chemisorbed species can be determined only through comparisons with the SHG response from a well-defined reference system. However, the use of SHG in this paper supports the electrochemical and spectroscopic evidence that there are a variety of ordered chemisorption processes occurring at all potentials on the well-ordered Pt(111) electrode surface, and that these processes differ from those observed on the Pt(100) and polycrystalline Pt electrodes. Future studies will address the structure of ordered monolayers of various anionic species at these surfaces.

ACKNOWLEDGEMENTS

The authors would like to thank P.N. Ross and J.D. McIntyre for helpful correspondence, and Jim G. Tobin for use of the Pt(100) crystal. The authors gratefully acknowledge the support of the National Science Foundation in these studies.

REFERENCES

1 (a) J. Clavilier, R. Faure, G. Guinet and R. Durand, J. Electroanal. Chem., 107 (1980) 205; (b) J. Clavilier, ibid., 107 (1980) 211.
2 (a) C.L. Scortichini and C.N. Reilley, J. Electroanal. Chem., 139 (1982) 247; (b) S. Motoo and N. Furuya, J. Electroanal. Chem., 172 (1984) 339.
3 F.G. Will, J. Electrochem. Soc., 112 (1965) 451.
4 A.T. Hubbard, R.M. Ishikawa and J. Katekaru, J. Electroanal. Chem., 86 (1978) 271.
5 P.N. Ross, Jr., J. Electrochem. Soc., 126 (1979) 67.
6 K. Yamamoto, D.M. Kolb, R. Kotz and G. Lehmpfuhl, J. Electroanal. Chem., 96 (1979) 233.
7 P.N. Ross, Jr., Surf. Sci., 102 (1981) 463.
8 F.T. Wagner and P.N. Ross, J. Electroanal. Chem., 150 (1983) 141.
9 M. Wasberg, L. Palaikis, S. Wallen, M. Kamrath and A. Wieckowski, J. Electroanal. Chem., 256 (1988) 51.
10 D.M. Kolb, Ber. Bunsenges. Phys. Chem., 92 (1988) 1175.
11 (a) K. Al Jaaf-Golze, D.M. Kolb, and D. Scherson, J. Electroanal. Chem., 200 (1986) 353; (b) J.D. McIntyre, private communication, 1989.
12 F.T. Wagner and P.N. Ross, Jr., J. Electroanal. Chem., 250 (1988) 301.
13 P.N. Ross in M.P. Soriaga (Ed.), Electrochemical Surface Science, Molecular Phenomenon at Electrode Surfaces, A.C.S. Symposium Series 378, American Chemical Society, Washington, DC, 1988, p. 37.
14 (a) D. Zurawski, L. Rice, M. Hourani and A. Wieckowski, J. Electroanal. Chem., 230 (1987) 221; (b) M. Hourani and A. Wieckowski, ibid., 227 (1987) 257.
15 A. Wieckowski, B.C. Schardt, S.D. Rosasco, J.L. Stickney and A. Hubbard, Surf. Sci., 146 (1984) 115.

16 N. Markovic, M. Hanson, G. McDougall and E. Yeager, J. Electroanal. Chem., 214 (1986) 555.
17 S. Chang, L. Leung and M.J. Weaver, J. Phys. Chem., 93 (1989) 5341.
18 A.T. Hubbard, J.L. Stickney, M.P. Soriaga, V. Chia, S.D. Rosasco, B.C. Schardt, T. Solomum, D. Song, J.H. White and A. Wieckowski, J. Electroanal. Chem., 168 (1984) 43.
19 J. Clavilier, J.P. Ganon and M. Petit, J. Electroanal. Chem., 265 (1989) 231.
20 L. Leung, A. Wieckowski and M.J. Weaver, J. Phys. Chem., 92 (1988) 6985.
21 (a) T.A. Driscoll and D. Guidotti, Phys. Rev., B28 (1983) 1171; (b) H.W.K. Tom, T.F. Heinz and Y.R. Shen, Phys. Rev. Lett., 51 (1983) 1983; (c) T.F. Heinz, M.M.T. Loy and W.A. Thompson, ibid., 54 (1985) 63; (d) H.W.K. Tom and G.D. Aumiller, Phys. Rev., B33 (1986) 8818.
22 S.G. Grubb, A.M. DeSantolo and R.B. Hall, J. Phys. Chem., 92 (1988) 1419.
23 (a) V.L. Shannon, D.A. Koos, S.A. Kellar, P. Huiang and G.L. Richmond, J. Phys. Chem., 93 (1989) 6434; (b) V.L. Shannon, D.A. Koos and G.L. Richmond, ibid., 91 (1987) 5548; (c) V.L. Shannon, D.A. Koos and G.L. Richmond, ibid., 87 (1987) 1440.
24 J. Miragliotta and T.E. Furtak, Phys. Rev., B37 (1988) 1028.
25 A. Friedrich, B. Pettinger, D.M. Kolb, G. Lupke, R. Stienhoff and G. Marowsky, Chem. Phys. Lett., 163 (1989) 123.
26 M.L. Lynch and R.M. Corn, J. Phys. Chem., 94 (1990) 4382.
27 (a) G.L. Richmond, J.M. Robinson, and V.L. Shannon Prog. Surf. Sci., 28 (1988) 1; (b) G.L. Richmond, Langmuir, 2 (1986) 132.
28 (a) R.M. Corn, M. Romagnoli, M.D. Levenson and M.R. Philpott, J. Phys. Chem., 81 (1984) 4127; (b) R.M. Corn, M. Romagnoli, M.D. Levenson and M.R. Philpott, Chem. Phys. Lett., 106 (1984) 30.
29 D.J. Campbell and R.M. Corn, J. Phys. Chem. 91 (1987) 5668.
30 (a) D.J. Campbell and R.M. Corn, J. Phys. Chem. 92 (1988) 5796; (b) D.J. Campbell, M.L. Lynch and R.M. Corn, Langmuir, in press.
31 J.E. Sipe, D.J. Moss and H.M. van Driel, Phys. Rev., B35 (1987) 1129.
32 P. Guyot-Sionnest, W. Chen and Y.R. Shen, Phys. Rev., B33 (1986) 8254.
33 Y.R. Shen, The Principles of Nonlinear Optics, Wiley, New York, 1984.
34 D.J. Campbell, D.A. Higgins and R.M. Corn, J. Phys. Chem., 94 (1990) 3681.
35 (a) T.F. Heinz, H.W.K. Tom and Y.R. Shen, Phys. Rev., A28 (1983) 1883; (b) Y.R. Shen, Nature (London), 337 (1989) 519.
36 B.C. Shardt, S. Yau and F. Rinaldi, Science, 243 (1989) 1050.
37 M.L. Lynch, B.J. Barner and R.M. Corn, in preparation.
38 W. Eberhardt, F. Greuter and E.W. Plummer, Phys. Rev. Lett., 46 (1981) 1085.